Experimental study of Si substitution by Ge in Ge-alloyed SiC epitaxial growth on 6*H*-SiC(0001)

M. Diani,[1] L. Kubler,[2,*] L. Simon,[2] D. Aubel,[2] I. Matko,[3] and B. Chenevier[3]
[1]*Département de Physique, Faculté des Sciences, Tétouan, Maroc*
[2]*LPSE, UMR CNRS-7014, Faculté des Sciences, 68093 Mulhouse Cedex, France*
[3]*Laboratoire des Matériaux et du Génie Physique, ENSPG, BP 46, 38402 St. Martin d'Hères, France*
(Received 22 July 2002; revised manuscript received 16 October 2002; published 28 March 2003)

The feasability of chemically modified heteroepitaxial growth on 6*H*-SiC(0001) has been investigated to contribute to band-gap engineering in SiC-based technology. A Ge-alloyed SiC:Ge epilayer has been grown on a 3×3 reconstructed surface, using repeated growth cycles. Each cycle included a low-temperature molecular-beam epitaxial atomic-layer supply of Si and Ge, followed by carbonization and annealing. The epilayer has been examined *in situ* by chemical and crystallographic surface analysis tools and *ex situ* by transmission-electron microscopy. The obtained chemical picture of the Ge uptake consists of a combination of bulk incorporation with buried Ge–C bond formation and a segregated part in the top layers, where Ge atoms are either bound to each other or bound to the Si atoms in excess on the 3×3 surface. On the basis of crystallographic local-order analyses, and in agreement with the presence of Ge-C bonds, we demonstrate that the bulklike Ge atoms substitute preferably to Si. The bulk fraction of the grown epilayer appears therefore as an $Si_{1-x}Ge_xC$ alloy with x less than 5%.

DOI: 10.1103/PhysRevB.67.125316 PACS number(s): 81.15.Hi, 79.60.−i, 64.75.+g, 61.14.−x

I. INTRODUCTION

During the last two decades, epitaxial growth of $Si_{1-x}Ge_x$ alloys on Si substrates has been a main breakthrough for the fabrication of quantum wells and superlattices and, hence, for band-gap and strain engineering in Si-based technology (see Refs. 1 and 2, and references therein). These alloys are well adapted to aid in the design of electronic devices. Metastable alloying of Si or Ge lattices with low carbon (C) contents to form either $Si_{1-y}C_y$ (Refs. 3 and 4) or $Ge_{1-y}C_y$ (Refs. 5 and 6) binary alloys, respectively, or C incorporation in SiGe alloys to form ternary epitaxial $Si_{1-x-y}Ge_xC_y$ alloys[7–10] (with y below 5%) has also been widely studied. Conversely and surprisingly, the incorporation of Ge in silicon carbide (SiC) to form SiC:Ge alloys has received very little attention so far in spite of similar and very promising potentialities. The latter alloys are actually no longer relevant for Si technology but are still very attractive for developments based on SiC. To date, only a few investigations have been made on Ge implantation in SiC, mainly motivated by the elaboration of heterostructured bipolar transistors based on SiC and Si:C Ge alloys.[11–13] The authors of these studies, who mention a band-gap reduction, essentially studied the electrical characteristics of the SiC:Ge materials, hence their structural properties remain largely unknown. Substitutional incorporation of Ge is admitted on the basis of a slight lattice expansion deduced from a shift of the SiC x-ray-diffraction peak,[11] but the question of whether Si or C is substituted by Ge in the SiC lattice has only been addressed theoretically by Guedj and Kolodzey.[14] They used a Keating model approach and, on the basis of energy calculations, concluded in favor of a preferential Si, rather than C, substitution by Ge. The latter case is less probable since it would give rise to larger local lattice distortions.

Two other studies,[15,16] using chemical vapor deposition (CVD) growth methods, have been devoted to Ge incorporation in SiC *grown on Si substrates*. The kinetic conditions used for these incorporations led these authors to apparent contradictory conclusions. For Mitchell, Spencer, and Wongchotigul,[15] Ge could not be incorporated into the grown film, with the Ge acting as a surfactant by surface segregation. For Sarney *et al.*,[16] a constant Ge incorporation throughout the film was preferably observed by secondary-ion-mass spectroscopy. We noticed that the Ge precursor flow in the CVD reactor was higher in the latter case.

Let us also mention recent experimental pioneering attempts of Ge incorporation into SiC lattices in order to form embedded Ge nanodots.[17,18] These attempts targeted strict phase separation between Ge and SiC by precipitation of Ge nanocrystallites in SiC. The topic of the present study is completely different since it is devoted to metastable, dilute, and random incorporation schemes of Ge atoms in a SiC lattice. The Ge concentrations must remain weak (below a few percent) like those achieved in doping processes or those maintaining a misfit compatible with epitaxial growth. In the present study our aim is to (i) obtain Ge incorporation in a SiC lattice by using molecular-beam epitaxial (MBE) growth and (ii) characterize the local environment of Ge atoms. Our purpose is therefore to experimentally investigate Ge substitution during SiC growth on SiC substrates and the possible Ge sites into an SiC lattice.

II. EXPERIMENT

The low desorption temperature of Ge on SiC and the high tendency of Si or Ge to cluster on this substrate make SiC alloys with Ge difficult to grow. The growth procedure will therefore require specific combinations of (i) low-temperature growth sequences, to trap or freeze individual Ge atoms into the bulk and (ii) higher-temperature steps, to rebuild an SiC lattice modified by the Ge incorporation. The

principle of the SiC:Ge crystal-growth process we develop here consists of three different sequences: by controlled MBE atomic-layer supplies, about two monolayers (ML) of Si added to small amounts of Ge (in a ratio defining the alloying) are first deposited at room temperature on a clean 3×3 reconstructed surface. A one-monolayer coverage (1 ML) is defined to be the ideal Si-atom density in an SiC(0001) plane, i.e., 1.22×10^{15} atoms/cm^2. This deposition step is followed by carbonization under C_2H_4 at 600 °C, providing the carbon required for the formation of two SiC bilayers, followed by annealing at 800 °C. These three steps define a growth cycle. Such cycles are repeated in order to build an SiC:Ge polytype structure by steps of about two bilayers or tetrahedral layer units. The low Ge concentration in the SiC:Ge alloy is monitored by the ratio of the Ge to Si ratio in the MBE flows. A similar process—without any Ge incorporation—has previously been recognized to result in an epitaxial $3C$-SiC formation onto $6H$-SiC substrates.[19]

The substrate surface preparation and the SiC:Ge depositions are carried out in an ultrahigh vacuum MBE chamber (10^{-10} mbar) equipped with *in situ* crystallographic and chemical characterization tools such as low-energy electron diffraction (LEED) and photoemission, respectively. The SiC:Ge alloy is grown on an Si-terminated face of a $6H$-SiC crystal obtained by the modified Lely method.[20] The (0001) face is initially cleaned *in situ* by native oxide desorption at 900 °C for 3 min under a weak MBE flux (around 5 Å/min) of atomic Si. As characterized by LEED, such a cleaning procedure leads to a (3×3) reconstructed surface on which the growth begins. To obtain one cycle of two atomic Si, Ge, and C bilayers (approximately 5-Å thick), Si and Ge are first deposited from Knudsen cells. This step is followed by a C supply and a thermal decomposition of C_2H_4. The total grown epilayer is about 85-Å thick and results from 17 identical sequential growth cycles. This growth process may be considered as a variant of atomic-layer epitaxy as previously reported.[21] Each Si and Ge deposition step (2 and 0.12 ML, respectively) on the (0001) plane of SiC is performed at room temperature to prevent any clustering or island formation. Clustering is indeed known to occur at higher temperatures in strongly strained Si/SiC heterostructures and leads to rapid island formation (Stranski-Krastanov mode).[22] A similar growth mode would likely also occur in further strained Ge/SiC interfaces, if the surface migration is not kinetically limited by a very low growth temperature. The preceding nominal Ge/Si ratio of incoming Ge and Si atoms ($x=12/200$ or 6%) was selected to limit the Ge bulk concentration [Ge/(Si+C)] in the finally formed SiC:Ge alloy to less than 3%. This Si-Ge deposition suppresses the LEED 3×3 pattern and is then carbonized at 600 °C by C_2H_4 molecules introduced via a leak valve into the UHV chamber. The substrate was at first maintained at room temperature. After pressure stabilization at 10^{-2} Pa, the sample was heated at 600 °C for 266 sec. This time corresponds to a reactive exposure to dissociating ethylene of 2×10^4 L (1 L $=1.33\times10^{-4}$ Pa×sec). The C amount supplied as a result of this method is much higher than that theoretically required to carbonize about 2 Si ML, but the sticking probability of C_2H_4 molecules is probably much lower than one. In addition, the dissociation rate is improved by cracking a part of the C_2H_4 molecules onto a hot W filament. Each growth cycle was followed by 2-min annealing at 800 °C. Annealing is expected to favor a 3×3 surface reconstruction and ensures good epitaxy. After *in situ* photoemission or LEED characterizations, the SiC:Ge layer stacking is finally capped by a protective 500-Å-thick Si amorphous layer deposited at room temperature. The cap layer enables subsequent sample thinning for *ex situ* cross-section transmission-electron microscopy (TEM) analyses as described in Ref. 19. Figure 1 is a schematic view of the described deposits.

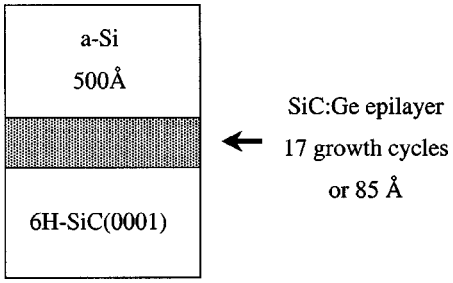

FIG. 1. Schematic view of the elaborated heterostructure.

Analyses that provide the main substance of the present study are surface chemical and crystallographic *in situ* controls by photoemission and LEED. Controls are performed throughout the cleaning procedure, within any growth sequence and all along the different growth cycles. Thus, surface chemical analyses by x-ray photoelectron spectroscopy (XPS) allow us to first control the surface cleanliness, follow the chemical evolution along the different SiC:Ge growth stages, and finally check the presence of Ge in the grown epilayer. Using a binding-energy shift analysis on Ge core levels, Ge-C chemical bonds could be differentiated from Ge-Si or Ge-Ge bonds. Conventional Mg K_α (1253.6 eV) and Al K_α (1486.6 eV) photon sources of a VG CLAM-100 spectrometer were used for XPS spectra recording. To achieve surface-sensitive conditions, grazing detection angles were used for the detection of the XPS spectra. XPS curve fitting is carried out using a standard Voigt function and a fit quality assessed by χ^2 minimizing. Linewidths of 1.5 eV and Voigt function parameters were kept constant throughout the analysis of Ge $3d$ related components in SiC.

X-ray photoelectron diffraction (XPD) allows *in situ* crystallographic characterizations and local order information around the incorporated Ge atoms. This technique is a by-product of XPS, i.e., namely it consists of angular-resolved, core-level intensity scans, in a given azimuthal plane, of a presumed monocrystal. More precisely, the crystallographic information is based on the observation of enhanced intensities along low index crystallographic directions, on experimental polar-angle (θ) distribution curves $I(\mathrm{C}\ 1s)$, $I(\mathrm{Si}\ 2p)$ (for pure SiC crystals) or $I(\mathrm{Ge}\ 3d)$ (in the present alloy) $=f(\theta)$, where θ is the electron emission angle with respect to the surface normal. These intensity angular peaks are essentially the consequence of forward scattering, along atomic row directions, of electrons emitted in the photoemission process. The concept of forward scattering is itself a simplified but realistic picture, for kinetic energies of the emitted

electrons in the 1-keV range, of the interference pattern between the directly emitted electron wave and those scattered by all surrounding atoms. The short-range-order character of the technique finally results from the limited (about 1 nm) elastic electron mean free path governing the coherent scattering at the origin of the XPD modulations. This principle is similar to that used in x-ray-absorption fine-structure analysis. The measured angular intensity modulations are therefore determined by the local structure around the emitter atom. Since the latter is selected by the choice of the scanned core level (C 1*s*, Si 2*p*, or Ge 3*d*), this technique is an element-specific, short-range-order probe of atoms around C, Si, or Ge atoms in the SiC:Ge network. In other words, the intensity peaks of a specific polar-angle distribution provide the real-space, crystallographic angular directions connecting a selected type of atom with its adjacent atom rows. XPD is therefore able to observe, for example, whether a collection of atoms is located in substitutional or interstitial lattice sites, with the first-neighbor atomic rows being different in both cases.

If applied, for instance, to the Ge 3*d* core level in an SiC:Ge alloy, this technique will be a short-range-order probe of the Ge atoms in the SiC lattice. In addition to being nondestructive, XPD has the advantage of enabling us to check the crystalline quality of the grown epilayer *in situ* at any time of the growth stage with a probing depth equivalent to that of an XPS analysis (a few tens of Angstrom, i.e., much higher than depths analyzed by LEED). After establishing the substitutional character of the Ge incorporation into the SiC lattice, Ge 3*d* angular distributions should also be able to provide information about the lattice sites (Si or C) of this substitution: depending on whether the Ge atoms occupy dominantly Si or C sites, these distributions will differ, since the chemical nature of the first-neighbor species will be inverted (C and Si, respectively). Actually, even in the case of identical geometrical locations of the first neighbors seen by a specific atom in the ZnS structure, the very different electron-scattering factors of C and Si strongly change the electron scattering,[23] and hence lead to differentiated XPD patterns when the chemical nature of these neighbors is inverted from C to Si. In other words, the Ge substitution site (Si or C) will be determined by its Ge 3*d* angular distribution: its resemblance to the Si 2*p* (or C 1*s*) distribution in the SiC lattice will signify that the Ge atoms meet the same chemical environment as does any atom in the Si (or C) sublattice, i.e., they occupy Si (or C) sites. This strategy will be applied here to determine the Ge substitution sites in the SiC lattice. More details about this technique can be found, for instance, in Refs. 19 and 23–26, dealing with the 3*C*- and 6*H*-SiC examples, and references therein. A main difficulty of such a study will nevertheless be the extraction of weak signal modulations from a minor population of Ge atoms limited to a few percent in the SiC matrix.

III. RESULTS AND DISCUSSION

A. Chemical analyses

Figure 2 shows XPS survey spectra taken first on the 6*H*-SiC substrate and after different growth cycles, corresponding to increasing SiC:Ge epilayer thicknesses. They represent the photoemission intensity as a function of binding energies referred to the sample Fermi level. In addition to the main Si 2*p*, Si 2*s*, and C 1*s* peaks of the clean SiC substrate [Fig. 2(a)], spectra in Figs. 2(b) and 2(c) exhibit Ge 3*d* (near 30 eV) and numerous Auger-Ge$_{LMM}$ (with a main peak located near 345 eV) features whose intensities increase with increasing epilayer thickness. A detailed description of the Si 2*p* and C 1*s* peak evolutions, specific to SiC growth, during the same growth procedure as described in the experimental part (but without any Ge supply), can be found in our previous study[19] with details on ethylene conversion in SiC. For each of these growth sequences, the binding-energy positions, lineshapes, and widths or intensities are not significantly modified by the present slight Ge incorporation.

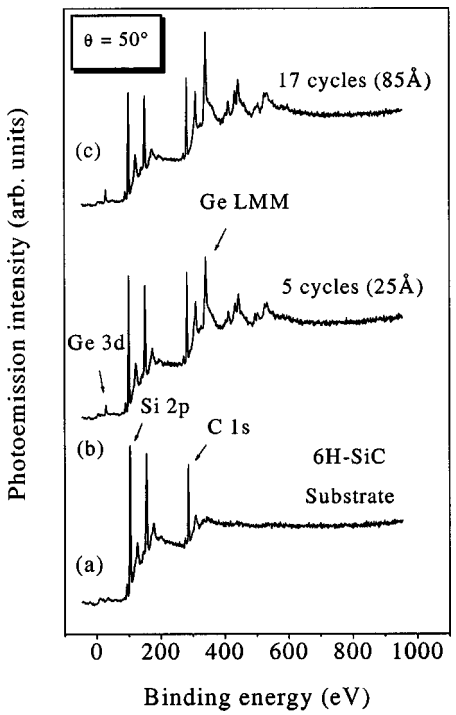

FIG. 2. XPS survey spectra, recorded with an Al K_α excitation source and taken (a) from a clean 6*H*-SiC(0001) substrate, (b) after five growth cycles of the SiC:Ge epitaxy (about 25 Å), and (c) after 17 cycles of the SiC:Ge epitaxy (about 85 Å).

Let us now focus solely on the features that characterize the Ge incorporation. The individual Ge 3*d* core levels on the left-side spectra of Fig. 3 are all taken at a normal electron emission angle after the last sequence (annealing at 800 °C) of different and indicated growth cycles. They highlight the Ge 3*d* intensity increase as a function of the number of deposition cycles or epilayer thicknesses. We notice that intensities are expected to be very weak at the first growth stages, since a maximal 3% concentration may nominally be incorporated in the beginning alloyed SiC epilayer. All these spectra clearly indicate the rising presence of Ge, either distributed in the bulk of the epilayer or segregated at its surface.

The Ge 3*d* core levels appear to be rather broad and may be resolved in two distinct components, located at 29.1 and

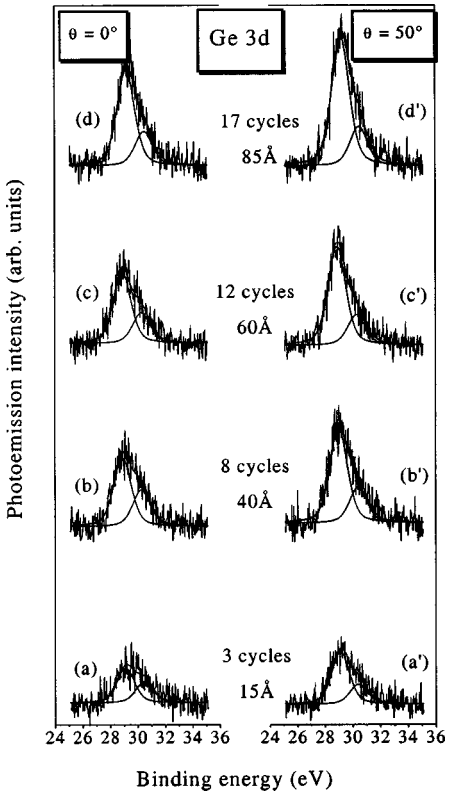

FIG. 3. Comparison along different growth cycles or SiC:Ge epilayer thicknesses (one cycle=5 Å) of XPS Ge 3*d* core levels, recorded at normal ($\theta=0°$) (left side) or grazing ($\theta=50°$) (right side) emission angles. Signals are resolved in two low and high binding-energy components.

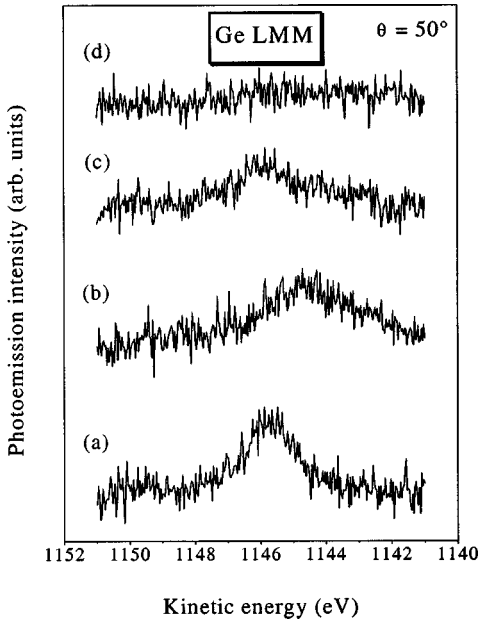

FIG. 4. Evolution of an XPS Ge_{LMM}-Auger peak along the different steps of a first attempt at SiC:Ge growth. The spectra are recorded at a polar angle of 50° (with respect to the surface normal) after (a) 2-ML Si and 0.12-ML Ge deposition at room temperature, followed by (b) a carbonization at 600 °C using a 2.10^4-L dose of C_2H_4 and (c) a 2-min heating at 800 °C restoring the 3×3 reconstruction, and (d) 900 °C annealing performed to desorb Ge.

30.4 eV, as obtained, for instance, after the third growth cycle. Ge atoms are thus in at least two different bonding states. The Ge chemical species that are candidates to describe our system are related to Ge-Ge, Ge-Si, or Ge-C bulk bondings and some possible surface-state bonds. Core-level shifts resulting from charge asymmetries of Ge surface states such as up and down dimers, have been recognized to be of the order of some tenths of electron volts[27,28] and cannot be responsible for the present large 1.3-eV shift. Concerning bulklike bonds, since Ge-Ge bonds exhibit a homopolar character and charge transfer in Ge-Si bonds is weak, the chemical shift or binding-energy difference between these two species is smaller than our spectrometer resolution. Therefore, these two species cannot be clearly differentiated nor, incidentally, at the origin of the chemical shift of 1.3 eV between the two observed subcomponents. Since C is significantly more electronegative than Si or Ge, Ge-C bonds must appear more heteropolar (Ge^+-C^-). The Ge 3*d* component of Ge bonded with C is thus expected to be found at a higher binding energy, with a local positive charge transfer on a Ge atom lowering the electron energy of the relevant core level. We therefore attribute the lower binding-energy component near 29.1 eV to Ge bound with itself or with Si, and the higher binding-energy component at 30.4 eV to Ge bound with C. The former attribution fairly fits our previous Ge 3*d* XPS analyses on $Si_{1-x}Ge_x$ alloys and on Ge layers deposited on Si. We had obtained Ge-Ge and Ge-Si bonds lying between 29.0 and 29.3 eV.[29] The attribution of the high binding-energy component agrees with previous XPS measurements of Amjoud *et al.*[30] on amorphous Ge_xC_{1-x} alloys. They found a similar shift toward 30 eV for a material presenting Ge-C bonds with respect to the binding energy of pure Ge-Ge bonds.

The origin of these two components may be further clarified and their attributions made more reliable if a Ge level is recorded along each step of a first attempt at a SiC:Ge formation cycle. Ge_{LMM}-Auger peaks, more intense than the Ge 3*d* peaks, have been chosen for this study. The step were previously described in Sec. II, and the relevant spectra are shown in Fig. 4. They reflect the significant chemical changes of the Ge atoms at the surface along an elementary growth cycle. After a room-temperature 2-ML deposition of Si and 0.12-ML Ge upon the Si-rich 3×3 surface and prior carbonization, a main and rather broad low binding-energy (or high kinetic-energy) component is observed as expected from the exclusive formation of undifferentiated Ge-Si or Ge-Ge bonds. After C supply and carbonization at 600 °C, this feature shifts towards higher binding-energy values, in agreement with a dominant conversion of the previous bonds into Ge-C bonds. Surprisingly, after annealing for two minutes at 800 °C, in addition to a renewed partial chemical shift, the previous amount of chemisorbed Ge seems to decrease slightly. This trend is confirmed by further annealing at 900 °C, where the Ge contribution completely disappears. This indicates that high-temperature treatments (above 800 °C) favor Ge desorption and that, as soon as temperature reaches 800 °C, a weak part of the Ge flow may not be in-

corporated into the bulk because of this desorption or sublimation at the surface. The annealing temperature has thus to be limited to 800 °C in the epitaxy procedure. Let us note that lower annealing temperatures would be unable to regenerate the surface crystallography.

In addition to partial desorption, by comparing spectra taken after carbonization, either before [Fig. 4(b)] or after [Fig. 4(c)] 800 °C annealing, it is possible to visualize a renewed chemical shift and transfer from Ge-C bonds to Ge-Ge or Ge-Si ones. This is the signature of a partial restoration of the initial bonding situation that occurred prior carbonization, after deposition at room temperature. Since a main part of the deposited elemental Si has been converted in SiC at 600 °C, the restoration of Ge-Ge or Ge-Si bonds can only be interpreted as the sign of a partial Ge segregation in the topmost layers at the SiC surface, newly formed at 800 °C. Recrystallization gives a partial Ge out-diffusion from the Ge-C bonds to the surface. Once the Ge signal has been weakened, either by desorption or by burrying into SiC, the left atoms are now probably bound with the restored Si-rich 3×3 layer. Since this scenario is probably repeated at each growth cycle, the two Ge features resolved after several growth cycles (as displayed in Fig. 3) actually stand for both a floating segregated Ge part and a bulk-distributed Ge-C component. Segregated Ge gives a component at low binding energy. Distributed Ge-C would contribute at higher energy and would really take part in the SiC alloying. Such a behavior may be explained by considering that the nominal Ge concentration is probably in excess of the bulk solubility in SiC at the formation temperature and is forced to remain or segregate at the surface.

This attribution of the two Ge subcomponents is further strengthened by changing the probing depths of the analyses. This is obtained by varying the electron emission angle. Thus, by comparing the right-hand series of spectra in Fig. 3, recorded at a more grazing electron emission angle (50°) with those taken at normal emission, it is possible to discriminate top-layer and bulklike contributions. The grazing analysis is more sensitive to surface-related components whereas bulklike components are more easily observed in normal analysis. Whatever the observed growth cycle, the Ge $3d$ intensity ratio of low and high binding-energy subpeaks increases significantly as the recording is varied from a normal (left side of Fig. 3) to a grazing emission angle (right side). This observation unambiguously indicates that the former component is more surface sensitive. The second one is attributed to the Ge-C bonds and is more bulk distributed.

Although obtaining quantitative values for the respective components is difficult, it is possible to obtain rough estimations by using oversimplified models incorporating ill-known sensitivity factors and electron attenuation lengths: the Ge $3d$ intensity corresponding to the segregated part increases rapidly with initial film growth but nearly saturates after the eighth cycle. This raises interesting, surface-science-specific questions, regarding the possibility of forming ordered 3×3 reconstructions on SiC(0001) by mixing Ge atoms with the Si in the top layer. Nevertheless, they are not the point of this study. After the last 17th cycle the corresponding Ge surface coverage is estimated to be 0.4 ML and the surface reconstruction becomes severely degraded. The bulk concentration of the burried Ge is still more uncertain. Keeping in mind that the total nominal Ge supply to the epilayer is 17 times 0.12 ML, i.e., about 2 ML, after subtraction of the previous segregated part (0.4 ML), a maximal value of 1.6 ML still has to be distributed in the bulk alloy. Since the whole epilayer is formed by 17×4 crystallographic (0001) planes, the distribution of the 1.6 ML of Ge into 68 planes defines a mean bulk concentration of $1.6/17\times4=2.5\%$ as referred to all Si+C atoms, or 5% as referred to the sole Si amount. Taking into account a possible and small desorbed Ge part, these values maximize the real Ge fraction in the SiC lattice. The electron attenuation inherent to the bulk distribution makes the corresponding XPS intensity lower than the segregated surface part (Fig. 3).

The first chemical picture of the Ge uptake we can therefore derive from all these observations consists of a subsurface incorporation with buried Ge-C bond formation. It coexists with a segregated part in the top layers, where Ge is either bound with itself or, more probably, with the Si excess of the 3×3 surface. This finding seems to result from the kinetic growth conditions we used. It also conciliates the apparently opposite behaviors observed in Refs. 15 and 16, where either low or high growth kinetics had been used. These studies favored either exclusive surface segregation or bulk incorporation schemes, respectively. Since we found the buried part to be associated with Ge-C bonds in a SiC lattice, Si substitution by Ge atoms is likely to occur. In the next section, we demonstrate this substitution scheme on the basis of crystallographic local order analyses.

B. Crystallographic order

In addition to the preceding chemical surface investigations, the crystalline quality of the epilayer has also been probed. We have first to quote our previous research,[19] in which a similar growth process was applied and resulting samples, free of Ge incorporation, were characterized by XPD, TEM, and transmission-electron diffraction. As samples were processed at low temperature, the heteropolytypic growth of a single $3C$-SiC phase on $6H$-SiC was obtained. A Moiré-fringe periodicity observed in high-resolution images was attributed to twinning in the grown $3C$ crystal. These defects resulted from three orientation possibilities to orient the $3C$-SiC structure in coincidence with the hexagonal substrate. A similar TEM investigation on the present SiC:Ge layer showed that the weak alloying does not modify the overall previous[19] SiC growth scheme. TEM images, with similar Moiré fringes, still ascertained an epitaxial relationship with the same associated twin defects, but since no Ge-related difference could be observed, these TEM images were not repeated here.

Ex situ TEM measurements also confirmed *in situ* indications of more or less faulty epitaxial growth, which were provided during growth by 3×3 LEED pattern restoration after each annealing at 800 °C at the end of each growth cycle. Such 3×3 LEED patterns have been discussed and displayed before[25,31] and we recall that their restoration follows their temporary disappearance after the Si+Ge MBE

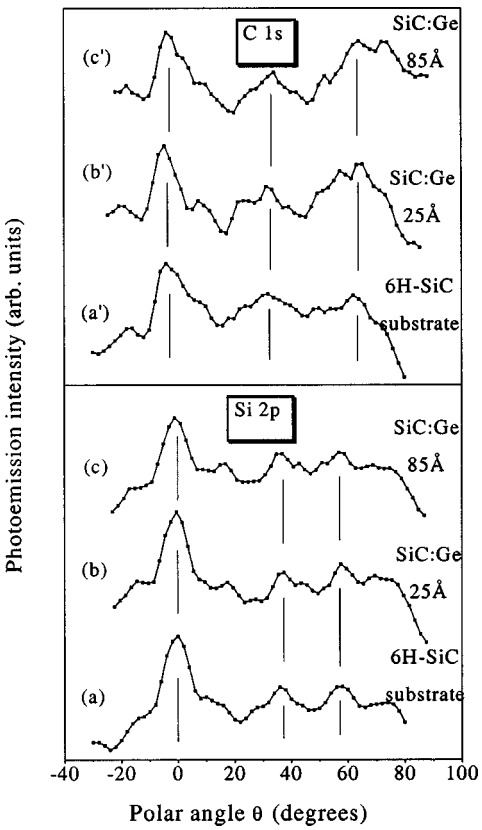

FIG. 5. Polar-angle XPD intensity modulations taken by using a Mg K_α excitation source for (from bottom to top) the Si $2p$ (a)–(c) and C $1s$ (a′)–(c′) core levels for the initial 3×3 $6H$-SiC substrate [(a) and (c)] and for the epilayer after 5 (25 Å) [(b) and (b')] and 17 (85 Å) [(c) and (c')] growth cycles, respectively.

deposition sequence at room temperature. With or without Ge incorporation, it may therefore be concluded that the low-temperature growth process used leads to a faulted $3C$ growth onto the $6H$-SiC substrate. Since the main topic of this study is the question of Ge short-range order in an SiC substrate, we will not further develop these questions of long-range crystal quality. Actually, the polytype change and the local incorporation scheme of the Ge atoms are probably two separate problems.

XPD is another powerful technique to probe epitaxy. As explained in Sec. II, it operates nevertheless *in situ*, between different growth cycles, and in a nondestructive way. This XPS subtechnique is, in addition, unique in that it is a short-range-order probe and better suited to providing information concerning the local crystallographic environment (first orders of next-nearest neighbors) of Ge atoms in SiC lattice sites. In this respect, XPD is complementary to TEM, which is more sensitive to detect longer-range crystal modifications and discriminate among $3C$ and $6H$ polytypes.[19] However TEM is not chemically selective and is unable to provide such local order information around incorporated Ge atoms.

Figure 5 shows the relevant XPD modulations, recorded for the Si $2p$ and C $1s$ core levels from the $6H$-SiC substrate and the SiC:Ge epilayer after 5 and 17 growth cycles. All these XPD patterns are taken in the same azimuthal plane. The first clear trend evident in Fig. 5 is the overall maintenance of the modulations and the similarity between the main angular features of the $6H$-SiC(0001) substrate and those from the epilayer after different growth cycles, either for Si or C emitters. Owing to the final 85-Å epilayer thickness and a weaker XPS probing depth, the latter modulations [Figs. 5(c) and 5 (c′)] are typically characteristic of the epilayer and no longer of the substrate. Actually, the electron emission contrasts are not significantly damped, as would be the case for an ill-ordered polycrystalline growth. Since the distributions are similar to those of the substrate, the epitaxial relationship between the substrate and the Ge-alloyed overlayer is thus further strengthened even though the exact polytype of the epilayer cannot be ascertained since XPD is not very sensitive to long-range-order modifications. This overall similitude between epilayer and substrate signatures is nevertheless sufficient to demonstrate a main SiC epitaxial relationship, the slight differences in the fine structure accounting for polytype changes and twinning.[19] The details of the scattering features observed in Fig. 5 will not be discussed here. This is a long task that has been only partly addressed in previous works[19,23–26] and is outside the scope of the present study.

To probe the Ge local environment, it is sufficient to use these angular Si $2p$ and C $1s$ diagrams as fingerprints of the SiC structural atomic arrangement in the probed plane and compare them to the expected Ge $3d$ distributions in the same plane. The Ge $3d$ intensities being much weaker than the Si $2p$ and C $1s$ ones, the signal/noise ratio of the Ge $3d$ XPD data becomes too weak to be recorded in reasonable acquisition times if the electron counting is not amplified by a high electron pass energy (100 eV). Unfortunately, the resulting loss of linewidth resolution does not allow recordings of distinct Ge $3d$ surface and bulk subcomponents as indicated in Fig. 3, where a 20-eV pass energy has been used. The raw XPD Ge $3d$ modulations, as observed in Fig. 6(a) after eight growth cycles, therefore only reflect angular modulations of the whole Ge $3d$ signal. By comparison with Si $2p$ and C $1s$ modulations at the same growth stage [Figs. 6(f) and 6(g)], the raw contrasts of the Ge $3d$ modulations are much weaker. This is explained by taking into account that only the minor bulk part (at higher binding energy) of the Ge $3d$ signal (Fig. 3) is expected to be subjected to forward scattering. Actually, the main surface part of the signal at lower binding energy does not modulate since the segregated Ge atoms in the topmost layer have no scatterers lying above them in the direction of analysis. The present weak Ge $3d$ modulations are therefore only the result of the modulations of the minor Ge $3d$ high binding-energy subcomponent in the whole convoluted Ge $3d$ spectrum. Improved information may nevertheless be extracted from raw data by classical procedures of instrumental function processing as indicated in Fig. 6. To check that the obtained Ge $3d$ modulations of Fig. 6(c) are not noise generated, we have repeated all the preceding procedures for other growth cycles or different SiC:Ge thicknesses, particularly after 11 and 14 growth cycles [Figs. 6(d) and 6(e)]. The similarity between all these Ge $3d$ angular distributions validates our signal extraction procedure. These nearly common Ge $3d$ XPD distributions [Figs. 6(c)–6(e)] may now be compared to the Si

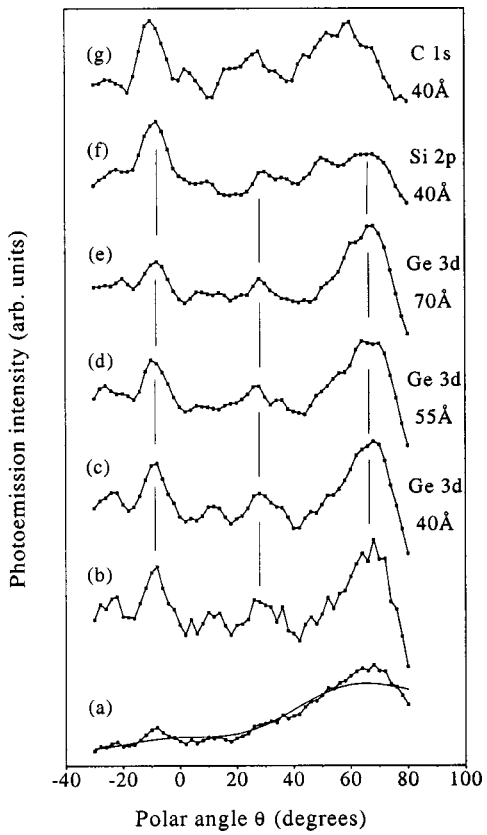

FIG. 6. Polar-angle XPD intensity modulations taken by using an Al K_α excitation source after eight growth cycles (40 Å) for the Ge 3*d* core level (a)–(c), compared to the Si 2*p* (f) and C 1*s* (g) distributions of the epilayer, recorded in the same plane. Raw data (a), raw data with instrumental function subtraction (b), and data fitted by a smoothing program (c) are, respectively, displayed for the Ge 3*d* modulations in order to extract better information. These preceding procedures have been repeated after 11 (d) and 14 (e) growth cycles (or for different SiC:Ge thicknesses) to check that the obtained Ge 3*d* modulation in (c) is not noise generated.

2*p* [Fig. 6(f)] and C 1*s* [Fig. 6(g)] patterns of the main elements of the alloyed epilayer. Clearly, they cannot account for the C 1*s* distribution but, owing to the complex signal extraction procedure, exhibit reasonable agreement with the Si 2*p* one. From these observations it is possible to conclude that the local environments of Ge and Si atoms in the SiC lattice are quite similar. This indicates that Ge substitutes preferably to Si in the SiC structure. In addition, a dominant incorporation of Ge atoms in, for instance, interstitial lattice sites may be excluded. Actually, the strongly modified local environment experienced by Ge atoms in hypothetical interstitial sites would not be compatible with the observed angular symmetry of Si-like patterns. The formed compound may therefore be described as an $Si_{1-x}Ge_xC$ alloy.

Finally let us note that our local order experiments report on Ge incorporation in an SiC lattice. The observed Ge substitution onto Si lattice sites, which is our main conclusion, is in good agreement with former energy calculations.[14]

IV. CONCLUSION

In this study we clearly demonstrate the feasability of Ge incorporation in an SiC matrix to form an SiC:Ge alloy. Incorporation is performed during MBE growth onto a 6*H*-SiC substrate using a low-temperature atomic-layer-epitaxy method. This method is necessary because Ge exhibits a strong tendency to cluster on SiC near 500 °C and sublimate above 800 °C. By careful chemical and crystallographic local order investigations by XPS and XPD, respectively, Ge atoms buried in the bulk of the grown epilayer are found to be bound to carbon atoms and to substitute onto Si lattice sites of the SiC crystal. Another fraction of the Ge amount segregates at the growth surface and is not bound to carbon. Regardless of this part of Ge floating at the surface, the bulk of the alloy that we have grown can be seen as an $(Si_{1-x}Ge_x)C$ alloy. Owing to a nominal 6% Ge supply (with respect to Si), the maximum *x* fraction incorporated into the bulk would be less than 5% once the segregated surface component and a possible desorbed part are subtracted. Even if these results suggest a possible breakthrough for differentiating heterostructures in SiC technology, their applications seem still limited by rather poor crystalline quality resulting from twin defects. This latter effect is similar to that observed in 3*C* growth onto 6*H*-SiC if growth temperature is close to that used in this work. These results may therefore open the route for band-gap engineering by using chemically modified heterostructures on SiC substrates provided that some remanent bottlenecks of quality SiC epitaxial regrowth are resolved.

ACKNOWLEDGMENTS

The authors are pleased to thank R. Madar and E. Pernot (ENSPG, Grenoble, France) for providing the 6*H*-SiC substrates.

*Corresponding author. Email address: L.Kubler@uha.fr

[1] E. Kasper and F. Schäffler, *Group IV Compounds Semiconductors and Semimetals*, edited by T. P. Pearsall (New York, Academic, 1991), Vol. 33, pp. 223–309.

[2] G. Abstreiter, P. Schittenhelm, C. Engel, E. Silveira, A. Zrenner, D. Meertens, and W. Jäger, Semicond. Sci. Technol. **11**, 1521 (1996).

[3] S. S. Iyer, K. Eberl, M. S. Gorsky, F. K. LeGoues, J. C. Tsang, and F. Cardone, Appl. Phys. Lett. **60**, 356 (1992).

[4] L. Simon, L. Kubler, J. Groenen, and J. L. Balladore, Phys. Rev. B **56**, 9947 (1997).

[5] J. Kolodzey, P. A. O'Neil, S. Zhang, B. A. Orner, K. Roe, K. M. Unruh, C. P. Swann, M. M. Waite, and S. I. Shah, Appl. Phys. Lett. **67**, 1865 (1995).

[6] M. Todd, J. Kouvetakis, and D. J. Smith, Appl. Phys. Lett. **68**, 2407 (1996).

[7] J. L. Regolini, S. Bodnar, J. C. Oberlin, F. Ferrieu, M. Ganneau, B. Lambert, and P. Boucaud, J. Vac. Sci. Technol. A **12**, 1015 (1994).

[8] S. C. Jain, H. J. Osten, B. Dietrich, and H. Rücker, Semicond. Sci. Technol. **10**, 1289 (1995).

[9] K. Eberl, K. Brunner, and O. G. Schmidt, in *Germanium Silicon*

Science and Technology, edited by R. Hull and J. C. Bean (1998).
[10] Y. Kanzawa, T. Saitho, and M. Kubo, Appl. Phys. Lett. **78**, 2515 (2001).
[11] G. Katulka, C. Guedj, J. Kolodzey, R. G. Wilson, C. Swann, M. W. Tsao, and J. Rabolt, Appl. Phys. Lett. **74**, 540 (1999).
[12] G. Katulka, K. Roe, J. Kolodzey, G. Eldridge, R. C. Clarke, C. P. Swann, and R. G. Wilson, Appl. Surf. Sci. **175–176**, 505 (2001).
[13] K. J. Roe, G. Katulka, J. Kolodzey, S. E. Saddow, and D. Jacobson, Appl. Phys. Lett. **78**, 2073 (2001).
[14] C. Guedj and J. Kolodzey, Appl. Phys. Lett. **74**, 691 (1999).
[15] S. Mitchell, M. G. Spencer, and K. Wongchotigul, Mater. Sci. Forum **264–268**, 231 (1998).
[16] W. L. Sarney, M. C. Wood, L. Salamanca-Riba, P. Zhou, and M. Spencer, J. Appl. Phys. **91**, 668 (2002).
[17] G. Hess, A. Bauer, J. Kräusslich, A. Fissel, B. Schröter, W. Richter, N. Schell, W. Metz, and K. Goetz, Thin Solid Films **380**, 86 (2000).
[18] Ch. Schubert, U. Kaiser, A. Heller, W. Wesch, T. Gorelik, U. Glatzel, J. Kräusslich, B. Wunderlich, G. Hess, and K. Goetz, J. Appl. Phys. **91**, 1520 (2002).
[19] M. Diani, L. Simon, L. Kubler, D. Aubel, I. Matko, B. Chenevier, R. Madar, and M. Audier, J. Cryst. Growth **235**, 95 (2002).
[20] Y. M. Tairov and V. F. Tsevtkov, J. Cryst. Growth **43**, 209 (1978).
[21] T. Fuyuki, T. Yoshinobu, and H. Matsunami, Thin Solid Films **225**, 225 (1993).
[22] A. Fissel, K. Pfennighaus, and W. Richter, Appl. Phys. Lett. **71**, 2981 (1997).
[23] S. Juillaguet, L. Kubler, M. Diani, J. L. Bischoff, G. Gewinner, P. Wetzel, and N. Becourt, Surf. Sci. **339**, 363 (1995).
[24] J. L. Bischoff, D. Dentel, and L. Kubler, Surf. Sci. **415**, 392 (1998).
[25] L. Simon, J. L. Bischoff, and L. Kubler, Phys. Rev. B **60**, 11 653 (1999).
[26] B. Schröter, A. Winkelmann, and W. Richter, J. Electron Spectrosc. Relat. Phenom. **114**, 443 (2001).
[27] J. A. Carlisle, T. Miller, and T.-C. Chiang, Phys. Rev. B **49**, 13 600 (1994).
[28] T.-W. Pi, R.-T. Wu, C.-P. Ouyang, J.-F. Wen, and G. K. Wertheim, Surf. Sci. Lett. **461**, L565 (2000).
[29] D. Aubel, Ph.D. thesis, University of Haute Alsace, 1995.
[30] M. B. Amjoud, A. Reynes, R. Morancho, P. Mazerolles, and R. Carles, J. Phys. IV (France) **1**, C2-327 (1991).
[31] M. Diani, J. Diouri, L. Kubler, L. Simon, D. Aubel, and D. Bolmont, Surf. Rev. Lett. (to be published 2003).